OPTIMIZED DISCRETIZATION OF SOURCES IMAGED IN HEAVY–ION REACTIONS

David A. Brown and Pawe l Danielewicz

Imaging techniques are used in many diverse areas such as geophysics, astronomy, medical diagnostics, and police work. The goal of imaging varies widely from determining the density of the Earth's interior to reading license plates from blurred photographs to issue speeding fines. A typical linear imaging problem involves extracting a source from measured data, where the data is represented as the convolution of a kernel with a source. An example of this is imaging the angle averaged relative source function $S_{\mathbf{P}}(r)$ from the angle averaged two-particle correlation function, $C_{\mathbf{P}}(q)$, often measured in nuclear reactions [1]:

$$C_{\mathbf{P}}(q) - 1 \equiv \mathcal{R}_{\mathbf{P}}(q) = 4\pi \int dr r^2 \, K_0(q,r) \, S_{\mathbf{P}}(r) \; . \tag{1}$$

Here $\mathbf{P}$ is the total momentum of the particle pair and the angle averaged kernel K is is equal to [2]

$$K(\mathbf{q},\mathbf{r}) = \frac{1}{2} \int d(\cos\theta_{\mathbf{qr}}) \left(|\Phi^{(-)}_{\mathbf{q}}(\mathbf{r})|^2 - 1 \right) \; . \tag{2}$$

The wavefunction $\Phi^{(-)}$ describes the propagation of the pair from a cm separation $\mathbf{r}$ out to the detector at infinity, where relative momentum $\mathbf{q}$ is reached. In the semiclassical limit, the relative source $S_{\mathbf{P}}$ for any two particles represents the probability distribution for emitting the the two particles with a separation $\mathbf{r}$, in their center of mass.

On the face of it, imaging appears straightforward: in the case of the two--particle correlation function, one could just discretize $C_{\mathbf{P}}$ and $S_{\mathbf{P}}$ and invert the resulting matrix equation. However, in practice this may not work as small variations in the data, within statistical or systematic errors, can generate huge changes in the imaged source. Using our method of Optimized Discretization, we can produce stable images despite these variations. This method uses the experimental error and the behavior of the kernel, K_0, to enhance the resolution of the image where the image is more "trustworthy" and decrease sensitivity elsewhere. In this paper, we will summarize this method and its application to proton--proton and intermediate mass fragment (IMF) two--particle correlation functions. This work is discussed in more detail in [3].

Typically in an experiment, the angle averaged correlation function $C_{\mathbf{P}}$ is determined at discrete values of the magnitude of relative momentum $\{q_i\}_{i=1,\ldots,M}$. With each determined value $C_i^{\rm exp}$ some error ΔC_i is associated. We use this set of values $\{C_i^{\rm exp}\}_{i=1,\ldots,M}$ to determine the source function. On inserting a discretized form of S into Eq. (1), we find a set of equations for the correlation functions $\{C_i^{\rm th}\}_{i=1,\ldots,M}$, in terms of $\{S_j\}_{j=1,\ldots,N}$,

$$C_i^{\rm th} - 1 \equiv \mathcal{R}_i^{\rm th} = \sum_{j=1}^{N} K_{ij} \, S_j \; , \tag{3}$$

where the angle-averaged kernel, K_{ij}, is averaged over each bin in r: $K_{ij} = 4\pi \int_{r_{j-1}}^{r_j} dr \, r^2 \, K(q_i,r)$. The source

values may be searched for by a χ^2 minimization

$$\sum_{i=1}^{M} \frac{(C_i^{\rm th} - C_i^{\rm exp})^2}{\Delta^2 C_i} = \min . \tag{4}$$

If we do not constrain the space within which we search for $\{S_j\}_{j=1,\ldots,N}$, then a set of linear equations for the values follows from differentiating (4) with respect to $\{S_j\}_{j=1,\ldots,N}$,

$$\sum_{ij} \frac{1}{\Delta^2 C_i} \left(K_{ij}\, S_j - \mathcal{R}_i^{\rm exp}\right) K_{ik} = 0 . \tag{5}$$

This is a matrix equation which can be solved for S:

$$S = \left(K^\top\, B\, K\right)^{-1}\, K^\top\, B\, \mathcal{R}^{\rm exp} . \tag{6}$$

where $B_{il} = \delta_{il}/\Delta^2 C_i$.

The error in the extracted source can be calculated from (6):

$$\Delta^2 S_j = \left(K^\top\, B\, K\right)^{-1}_{jj} = \sum_\alpha \frac{(u_j^\alpha)^2}{\lambda_\alpha} . \tag{7}$$

Here u_j^α and λ_α are the eigenvectors and eigenvalues of the $N \times N$ matrix

$$\left(K^\top\, B\, K\right)_{kj} \equiv \sum_{i=1}^{M} \frac{1}{\Delta^2 C_i}\, K_{ik}\, K_{ij} = \sum_{\alpha=1}^{N} \lambda_\alpha\, u_i^\alpha\, u_j^\alpha . \tag{8}$$

We see immediately that the error on the source diverges if one or more of the eigenvalues λ_α approaches zero. This might happen for any number of reasons, for example, when K_0 maps a region of the source to zero. Furthermore, it may happen that K_0 is approximately constant in some region, so it smoothes over the source, resulting in a loss of information. If we then try to restore S, we find that we cannot restore S uniquely at a high resolution. However, we still may be able to restore it at a lower resolution.

In other imaging applications, these problems are typically avoided by imposing constraints such as a positivity or smoothness on the source. In nuclear imaging we may actually want to *test* whether the source actually obeys such a constraint, so we would like a method that yields reliable results without the need for constraints. We have found that, by rebinning the source and the kernel, we can resolve the resolution issue and obtain a stable image without additional constraints. We do this by choosing the discretization of the source and the kernel to minimize the error in the source relative to some model source:

$$\sum_{j=1}^{N} \left| \frac{\Delta S_j}{S_j^{\rm mod}} \right| = \min . \tag{9}$$

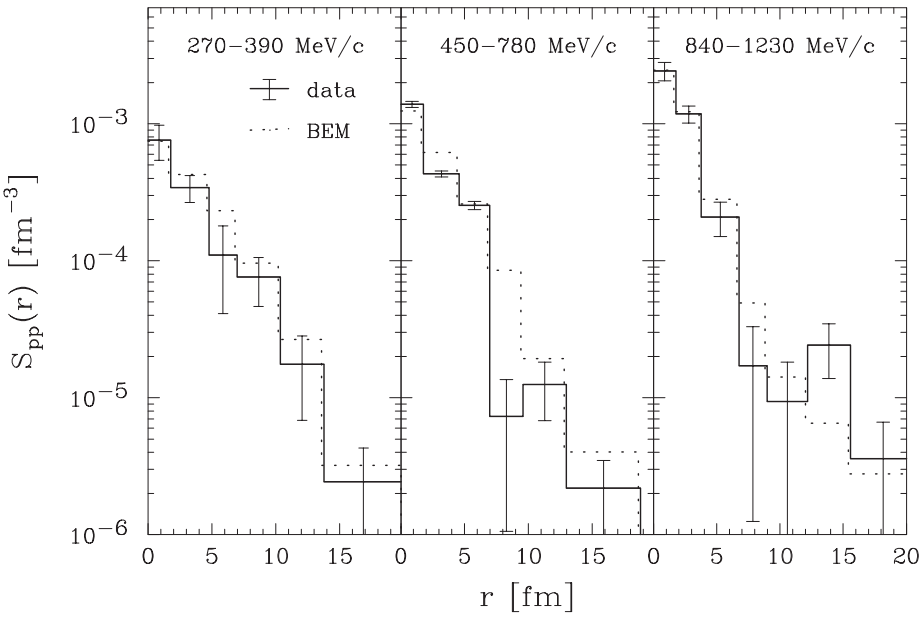

Figure 1: Relative proton source for pairs emitted from the $^{14}N + ^{27}Al$ reaction at 75 MeV/nucleon, in the vicinity of $\theta_{\rm lab} = 25°$ in the indicated pair momentum intervals. Solid lines are the sources we extracted from the data [4] and the dotted lines are the sources we obtained using the Boltzmann−equation calculation.

The actual shape of the model source is not important, provided that it is large where we expect the source to be large and small where we expect it to be small; we typically use a simple exponential model source.

Now we apply our Optimized Discretization method to analyze the pp correlation data [4], from the ^{14}N + ^{27}Al reaction at 75 MeV/nucleon. In the proton-proton (pp) case, the angle and spin averaged kernel is [1]

$$K_0(q,r) = \frac{1}{2}\sum_{js\ell\ell'}(2j+1)\,\left(g_{js}^{\ell\ell'}(r)\right)^2 - 1\,, \tag{10}$$

where $g_{js}^{\ell\ell'}$ is the radial wave function with outgoing asymptotic angular momentum ℓ (We also apply the constraint that the norm of the source is ≤ 1 within the imaged region; since the source is normalized to 1 when integrated over all space [1], this constraint simply eliminates impossible sources from consideration). We compare the pp sources from the data to those from the transport model [5], over a large range of relative separations and magnitude of the sources. Past experiences in comparing semiclassical transport models to single-particle and correlation data have been mixed [4, 8, 9, 10], for this particular reaction and others in this energy range.

In Fig. 1, we compare the images extracted from the data to the distributions of relative separation of last collision points for protons with similar momentum from the transport model [1, 5]. Generally, the Boltzmann-equation model (BEM) yields relative emission point distributions that are similar to the imaged data, including the dependence on total pair momentum. This finding is somewhat surprising for the low and intermediate total momentum intervals. While BEM adequately describes high-momentum wide-angle single-particle spectra of protons, which correspond to the highest total-momentum interval (see Fig. 1 in [8]), the model overestimates the single-particle proton spectra by as much as 1.5-5 in the two lower momentum intervals [8]. Looking closer at Fig. 1, we find that the distributions from data are somewhat sharper at low-r in the two lower total-momentum intervals than the the distributions from

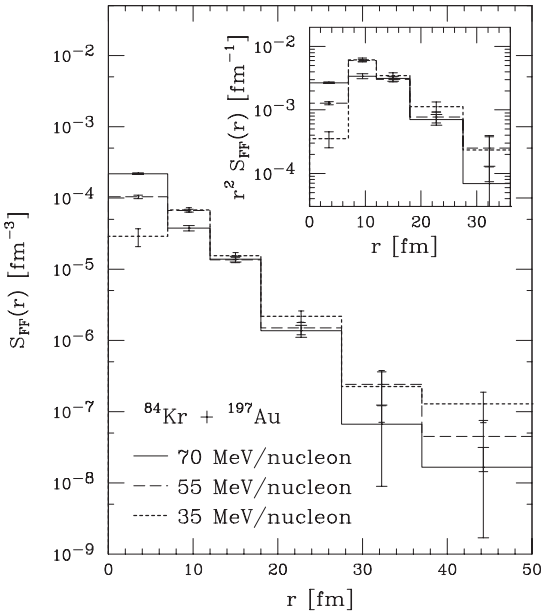

Figure 2: Relative source for IMF's emitted from central $^{84}Kr + ^{197}Au$ reactions from the data of Ref. [6] for the indicated beam energies. The inset shows the source multiplied by r^2. In both plots, the full image extends out to 90 fm.

the model. We see an even greater disagreement between the data and the model when we compare the integrals of the source in the BEM and the data. We find that only 55%-70% (depending on the momentum interval) of the strength of the sources lies within the imaged region in the data, while BEM predicts that 90%-98% of the strength should lie in this range. This implies that many protons are being emitted at large distances, outside the range of the image, and that BEM produces the protons to close to the decaying remnant.

The Optimized Discretization method can be applied equally well to IMF sources. We choose the correlation data of Hamilton *et al.* [6], from central ^{84}Kr + ^{197}Au reactions at 35, 55, and 70 MeV/nucleon, because these data allow us to examine the variation of sources with beam energy. Pairs were collected in the angular range of $25^\circ < \theta_{\rm lab} < 50^\circ$ in order to limit contributions to the correlation functions in [6] from target-like residues. Hamilton *et al.* tabulate the functions in terms of the reduced velocity $v_{\rm red} = v/(Z_1 + Z_2)^{1/2}$, under the assumptions that the Coulomb correlation dominated the fragment correlation and that the fragments were approximately symmetric, $Z/A \approx 1/2$.

When we invert this data, we work in the classical limit of correlations of purely Coulomb origin, such as investigated between the IMFs in [7]. In this case, the kernel is

$$K_0(q,r) = \theta(r - r_c)\ \left(1 - r_c/r\right)^{1/2} - 1\,. \tag{11}$$

Here the distance of closest approach for symmetric fragments is approximately $r_c \approx e^2/m_N\, v_{\rm red}^2$. To image of the IMF sources, we optimize $\{r_j\}_{i=1,\ldots,N}$ as in the pp case, but we add the constraint $r_1 \geq r_1^{\rm min}$. We do this because the Coulomb interaction in (11) does not dominate when the measured fragments are in close contact. The Coulomb correlation alone cannot be relied upon to get information on the most inner portion of the source. The typical touching distance for the fragments measured in [6] is $r_t \sim 5$ fm; we chose a value $r_1^{\rm min} = 7.0$ fm which ensures that there is more volume in the lowest bin outside r_t, than inside r_t.

The results from the imaging are shown in Fig. 2. Given the errors in the figure, the tails of

the sources at the three energies are not very different. However, we observe significant variation with energy at short relative distances ($r < 12$ fm) with the source undergoing a larger change between 55 and 75 MeV/nucleon, than between 35 and 55 MeV/nucleon. We also see that a large part of IMF emission occurs at distances that are not imaged with the protons. This is simply because the IMF kernel is more sensitive to the large r regions of the source. We find that over 96% of the IMF sources are within 50 fm but only 72-79% are within 20 fm.

The tails of the IMF sources extend so far that they must be associated with the time extension of emission. Even so, it is interesting to ask how far into the center of the source must we go to see where the effects due to the spatial extent of the primary source. In [6], the combinations of single-particle source radii and lifetimes that gave acceptable descriptions of their data have radii varying between 5 and 12 fm. With this, one could try to separate the temporal and spatial effects using a three-dimensional source restoration. In the angle-averaged source, the part dominated by lifetime effects should fall off as an exponential divided by the square of the separation, r^2, as a function of relative separation. On the other hand, the part of the relative source dominated by spatial effects may fall off at a slower pace or even be constant. In Fig. 2, we see that the sources change weakly with r at 35 and 55 MeV/nucleon and faster at 70 MeV/nucleon, within the range where sources vary with energy ($r \lesssim 12$ fm). For reference, in the insert to Fig. 2 we show the IMF source multiplied by r^2. We see an edge at $r \sim 11$ fm at 35 and at 55 MeV/nucleon which disappears at 70 MeV/nucleon. This is consistent with an emission from the spatial region of a radius $R \sim 11/\sqrt{2} \sim 8$ fm that becomes more diffuse, and possibly spreads out, with the increase in energy. The disappearance of the sharply pronounced spatial region at 70 MeV/nucleon agrees with the general expectation on the IMF production in central symmetric collisions or from central sources in asymmetric collisions that the IMF yields maximize towards 100 MeV/nucleon [13].

We have introduced the new method of optimized discretization to image sources. This method is suitable for determining the relative source from different particle pair correlations in heavy-ion collisions. Recognizing the need for stable imaging, in our method we adjust the resolution to minimize the relative errors of the source. This new method allows one to study the *long-range* source structure by adjusting the overall size of the imaged region and the resolution at large distances.

We found that our imaged pp sources change significantly with the total pair momentum, becoming sharpest for the largest momenta in the cm. Significant portions of the imaged source are missing from the imaged region at typical participant momenta in the cm, but not at the highest momenta. The integral of the source in the Boltzmann-equation model [11, 5] agrees with the data, at the highest momenta but the integral is close to one in the participant and target-emission momenta. Gaussian-source fits to the height of the pp correlation function [12, 4] are of a limited value because considerable source strength may lie at large relative separations. In our analysis of midrapidity IMF sources in central ^{84}Kr + ^{197}Au reactions at different beam energies, we found a significant variation of the sources with energy at short distances, but not at large distances. Considerable portions of the IMF sources extend to large distances ($r > 20$ fm) just like the lower total-momentum pp sources. It would be very interesting to image both the IMF and pp sources in one reaction.

References

1. D. A. Brown and P. Danielewicz, Phys. Lett. B 398, 252 (1997).
2. S. E. Koonin, Phys. Lett. B 70, 43 (1977); P. Danielewicz and P. Schuck, *ibid.* 274, 268 (1992); S. Pratt, T. Csorgő, and J. Zimanyi, Phys. Rev. C 42, 2646 (1990).

3. D. A. Brown and P. Danielewicz, Phys. Rev. C 57, 2474 (1998).
4. W. G. Gong *et al.*, Phys. Rev. Lett. 65, 2114 (1990); Phys. Rev. C 43, 1804 (1991).
5. P. Danielewicz, Phys. Rev. C 51, 716 (1995).
6. T. M. Hamilton *et al.*, Phys. Rev. C 53, 2273 (1996).
7. Y. D. Kim *et al.*, Phys. Rev. Lett. 67, 14 (1991).
8. W. G. Gong *et al.*, Phys. Rev. C 47, R429 (1993).
9. D. Handzy *et al.*, Phys. Rev. Lett. 75, 2916 (1995).
10. S. Gaff *et al.*, Phys. Rev. C 52, 2782 (1995).
11. P. Danielewicz and G. F. Bertsch, Nucl. Phys. A 533, 712 (1991).
12. D. H. Boal, C. K. Gelbke, and B. K. Jennings, Rev. Mod. Phys. 62, 553 (1990).
13. W. Lynch, submitted to Reviews of Modern Physics, 1997.